DOI: 10.65731/ama/2026-0053

PERFORMANCE EVALUATION OF SMART HYBRID COMPOSITES INCORPORATING SHAPE MEMORY ALLOY ELEMENTS

Abdelaziz LEBIED*, Sidali BACHA*, Houssam LALA*, Mohamed Lakhdar SAHLI**

*Transport and Environment Engineering Laboratory, Transport Engineering Department,
Faculty of Science of Technology, Constantine 1- Frères Mentouri University, 25000, Algeria
**Normandie Univ, ENSICAEN, UNICAEN, CEA, CNRS, CIMAP, Université de Caen Normandie,
Montfoulon 61250 Damigny, France

Lebied.aziz@yahoo.fr, sidali.bacha@umc.edu.dz, lalahoussam4300@gmail.com, mohamed.sahli@unicaen.fr

received 02 April 2026, revised 21 July 2026, accepted 24 July 2026

Abstract: Smart materials such as shape memory alloys offer innovative solutions in industry, based on their main characteristic of returning to their initial shape after deformation, in response to a temperature difference. When SMAs are combined with other materials, they give rise to the formation of smart composites. The composites were manufactured from epoxy resin, reinforced with Ti-Ni SMA wires, by studying their mechanical properties. This study presents the stress-strain relationships of a composite incorporating SMA wires. The study highlights, in a first part, the impact of SMA wires on the mechanical behavior of a composite plate, then analyzes the adaptation capacity and reliability of hybrid shape memory composites.

Key words: composite materials, shape memory alloys, mechanical characterization, martensitic transformation, numerical analysis

1. INTRODUCTION

Over the past ten years, the field of smart materials and structures has witnessed a significant increase in interest, driven by their significant potential for scientific and technological breakthroughs [1–3]. The uses of these advanced materials are now remarkably diverse. Essentially, they are designed to detect changes in the environment and optimize their performance in an optimal way to achieve a specific goal. This means that when triggered by an external stimulus, they give a pre-programmed and precise response, and only return to their original form after the triggering event has ended [4-6].

This broad category includes many different classes of materials, all with unique properties that make them suitable for everything from revolutionary new technologies to common everyday products. These include: shape memory alloys, piezoelectric materials, electro-rheological materials, as well as chromic materials, which are capable of changing their color in response to various stimuli. Their ability to modify their properties in response to external stimuli constitutes an asset for the development of adaptive components, likely to improve the performance and reliability of materials used in structures.

Shape memory alloys (SMAs) constitute a distinct family within smart materials [7, 8]. They exhibit the property of deforming and returning to a programmed shape depending on temperature (Fig. 1). The thermoelastic martensitic transformation gives them the ability to generate high forces or large displacements [9–15].

The main characteristic of SMAs is their ability to memorize and restore their initial configuration once heated beyond their characteristic transition temperatures. [16–18] This behavior is explained by a phase transformation of their microstructure, passing from the martensitic state to the austenitic state upon reaching the transition temperature [19–21]. Thus, when a sample is stressed beyond the deformation necessary to induce this transformation, it can recover its deformation simply by unloading [22, 23].

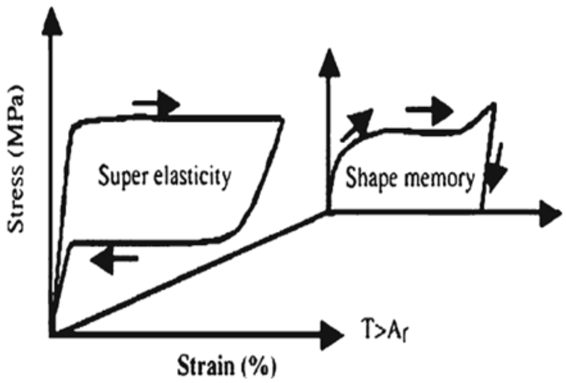

Fig. 1. The mechanism of the shape memory effect

In the SMA family, the Ti-Ni alloy occupies a predominant place due to its industrial use, especially in sensors and actuators. It is most often produced by foundry and forging processes. Ti-Ni constitutes an attractive reinforcement material for composites, combining a relatively low cost with remarkable properties [24–32]. Equiatomic (50/50) Ti-Ni alloys can transform at temperatures close to 0°C and exhibit exploitable superelasticity between 0°C and 250°C, making them excellent candidates for consumer electronic devices. In recent years, there has been increasing scientific interest in this special class of materials [8, 16, 33–37].

Composites reinforced with shape memory alloy fibers have notable advantages, ranging from increased strength and stiffness to improved buckling resistance and superior dynamic properties (Fig. 2). SMAs have found use as actuators, allowing efficient control of both large static deformations and structural vibrations [25, 38–40]. In addition, the compressive stresses generated during the martensite → austenite transformation make it possible to reduce the stress concentration in the vicinity of cracks and to slow down their growth by fatigue [25, 41, 42].

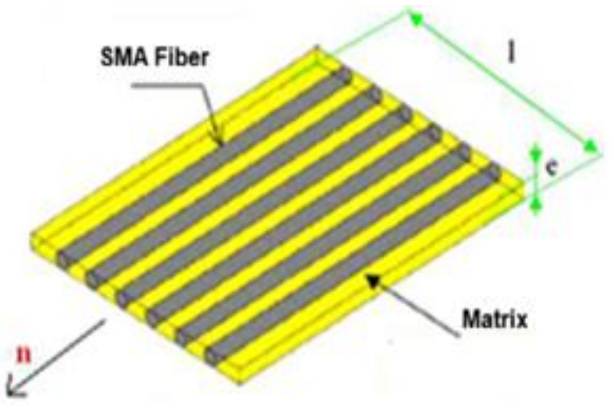

Fig. 2. Orthotropic Network-Reinforced Composite Plate

Composites reinforced with SMA fibers—applied to the substrate or inserted into resin sheaths—have been the subject of numerous investigations, synthesized in various literature reviews [4, 17, 44, 45]. They can be considered as having a certain intelligence, since the SMA wires act both as strain sensors and as reinforcing elements, thus contributing to improving the resistance at high temperatures. They can be considered as having a certain intelligence, since the SMA wires act simultaneously as strain sensors and reinforcing elements, thus improving the resistance at high temperatures (M_f), thanks to the rearrangement of the structure of the martensitic variants.

When the temperature exceeds A_f, the alloys undergo a phase transformation, evolving from the martensitic state to the austenitic state. During this transformation, the SMA wires regain their length. The development of residual stresses is a key element to increase the yield strength of the composite at high temperature. Based on this mechanism, specimens incorporating shape memory wires were fabricated. The essential performances and application areas of SMA composites, resulting from the combination of a shape memory alloy reinforcement and a polymeric or metallic matrix, have been extensively explored in the literature [46–48].

The development of laminated structures based on shape memory alloys and polymers is one of the notable contributions, offering the possibility to study the bending behaviors of hybrid composites [49–51]. Birman presented a detailed review study on the characterization and constitutive modeling of SMA, also highlighting their applications |43]. The analysis of the mechanical properties in thickness of quasi-isotropic smart carbon/epoxy laminates was carried out by Alam et al [48].

The research of Xue and Lee, [52] combining modeling and experimentation, highlighted the use of SMA wires to induce instantaneous buckling of non-symmetrical composite laminates. In their study, Zhang and Liu [47] investigated the free and forced vibrations of a large-strain composite plate incorporating SMA wires, using the thermomechanical constitutive model proposed by Mandolino and colleagues [48, 52, 53]. The experimental work of Patel et al. [46] highlighted the fracture behavior under uniaxial tension as well as the deformation response under thermomechanical loading of polycarbonate composites reinforced with Ti-Ni wires.

Despite the considerable advances made in the development of hybrid composite materials reinforced with shape memory alloys, several scientific and technological challenges still limit their use in demanding structural applications. One of the main difficulties concerns the quality of the interfacial adhesion between the SMA wires and the polymer matrix. This interface plays an essential role in the transfer of mechanical loads; [54] insufficient adhesion can lead to sliding phenomena, local decohesion, or delamination, thereby reducing the reinforcement efficiency and the durability of the composite [55].

Furthermore, the significant differences in elastic modulus, coefficient of thermal expansion, and phase transformation behavior between Ti–Ni alloys and polymer matrices give rise to thermomechanical incompatibilities that are likely to generate residual stresses during manufacturing and in-service operation [56]. These stresses can promote progressive interfacial damage and reduce the quality of load transfer between the constituents [57–58].

Moreover, the overall mechanical response of these composites strongly depends on numerous parameters, such as the prestrain of the SMA wires, their volume fraction, their orientation, the interface properties, and the thermomechanical activation conditions. This strong interdependence makes it difficult to achieve reliable and reproducible mechanical performance and actuation capabilities, which still represents a major challenge for the design of smart composite structures [59].

These limitations show that the understanding of load transfer mechanisms remains a major scientific challenge. In this context, the development of predictive numerical models requires a rigorous description of the constitutive laws of the constituents, of the wire/matrix interactions, as well as of the loading conditions. The reliability of such a model also depends on the quality of parameter identification and its experimental validation [60].

Beyond the challenges associated with interfacial bonding and load transfer, shape memory alloys (SMAs) exhibit an inherently complex thermomechanical behavior, characterized by hysteresis effects, reversible phase transformations, path-dependent responses, and the progressive evolution of material properties under repeated loading. During cyclic loading, martensitic transformations may evolve from one cycle to another, leading to changes in transformation stresses, a reduction in recoverable strain, and a gradual degradation of functional performance, a phenomenon commonly referred to as functional fatigue [60,61].

These mechanisms are now widely recognized as key factors in assessing the reliability and long-term durability of smart structures incorporating SMAs [62]. However, owing to the experimental complexity associated with their characterization, the present study deliberately focuses on the mechanical response under monotonic loading conditions. This choice provides a suitable framework for the development and validation of a numerical model capable of reproducing the initial behavior of the investigated hybrid composites. The analysis of cyclic behavior and long-term stability remains an important direction for future research [63].

In light of the challenges discussed above, several experimental and numerical approaches have been proposed to enhance the performance of SMA-reinforced hybrid composites [64,65]. Nevertheless, most existing studies primarily focus either on mechanical characterization or on conventional numerical modeling approaches, without providing a sufficiently detailed description of the interactions between SMA wires, the polymer matrix, and their interface. Furthermore, only a limited number of investigations

DOI: 10.65731/ama/2026-0053

combine the development of a numerical model specifically designed for intelligent hybrid composites with an experimental validation performed on specimens manufactured under the same processing conditions [66].

Within this context, the main contribution of the present work lies in the development of an original numerical model dedicated to reproducing the thermomechanical behavior of polymer-based hybrid composites reinforced with superelastic Ti–Ni wires. The proposed model is based on a phenomenological representation of SMA behavior and explicitly accounts for the mechanical interactions among the reinforcing wires, the polymer matrix, and the interfacial region. Its predictive capability is assessed through direct comparison with experimental results obtained from specimens specifically manufactured for this study. By combining experimental investigations with numerical simulations, the proposed approach provides an effective tool for improving the understanding of the mechanical response of smart composites and supporting their future design and optimization.

Although the present work is conducted on laboratory-scale specimens, the proposed methodology has been conceived as a first step toward the development of numerical tools dedicated to the analysis of larger-scale intelligent composite structures. The objective of this study is to develop and validate a numerical model capable of predicting the thermomechanical behavior of Ti–Ni wire-reinforced hybrid composites through an approach combining experimental testing and finite element simulations. The proposed framework aims to provide a predictive tool for the analysis and optimization of this class of smart structures.

In this context, the reliability of such a model depends not only on the adopted constitutive assumptions but also on the quality of parameter identification and their experimental validation. Accordingly, the present study adopts an integrated methodology combining experimental investigations and finite element modeling to establish a numerical framework capable of accurately reproducing the mechanical response of the investigated composites under monotonic loading conditions.

2. EXPERIMENTAL PROCEDURE AND MATERIALS

2.1. Materials

The composite was prepared using ER3 epoxy resin as the matrix and EH208W curing agent, manufactured by GHCRFT Co., Ltd., Japan. ER3 epoxy resin offered high impact resistance, with a Tg close to 140 °C. The physical and mechanical properties of Ti-Ni alloy and ER3 epoxy resin are shown in Table 1. In this study, the SMA wire used has a diameter of 0.2 mm; it is of Chinese origin and its composition is Ni-50.8 wt% Ti. A heat treatment at 870 °C for 30 minutes was applied to each wire, followed by quenching in water and holding for 2 hours. The end-of-austenite temperature after treatment is 79°C, the wires being martensitic at room temperature.

The micrograph is shown in Fig. 3a. The main physical properties of equiatomic Ti-Ni are given in Table 1. DSC analysis, interpreted by the tangent method, allowed to determine the transformation temperatures of the alloy: A_s = 50°C, A_f = 79°C, M_s = 58.4°C and M_f = 32.4°C [Fig. 3b]. The observations indicate that the initial reverse transformation temperature is higher for the deformed wire sample, compared to the undeformed one.

This phenomenon can be interpreted from the thermodynamic point of view: The deformation has the effect of releasing the elastic energy stored in the martensites of the polycrystalline SMA, energy which constitutes the driving force of the reverse martensitic transformation. [67] In addition, the plasticity of the alloy matrix has been suggested as another potential mechanism [68]. The matrix polymer was ER3 epoxy resin, while the curing agent used was EH208W, produced by GHCRFT Co., Ltd. [Japan]. ER3 epoxy resin had good thermal resistance and a tensile elongation at break of 12% up to Tg+50 °C. The base materials used in this study were Ti-Ni alloy and ER3 epoxy resin, the mechanical properties of which are shown in Table 1.

Tab. 1. Component mechanical properties

Properties	SMA austenitic 100 %	SMA martensitic 100 %	Epoxy
Young's modulus [GPa]	70	20	2.5
Density [g/cm³]	6.45	6.45	1.15
Poisson's ratio	0.33	0.33	0.35
Glass temperature [°C]	-	-	120

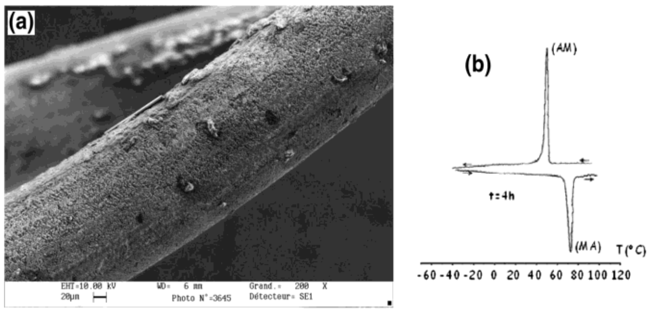

Fig. 3. (a) The Surface Properties of MA Wire at 20°C; (b) Thermal Analysis of Annealed Ti-Ni [650 °C, 4 h]

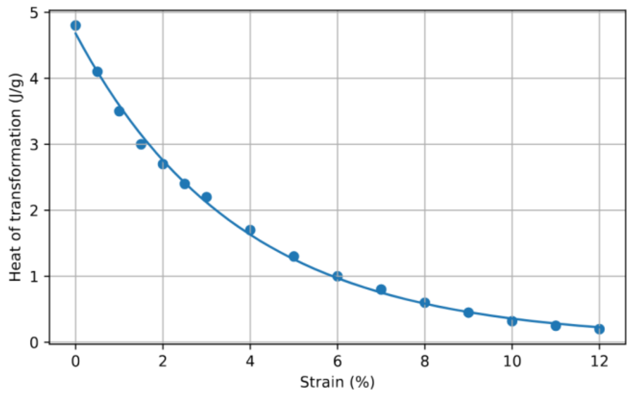

Fig. 4. Transformation Enthalpy of Ti-Ni Wires as a Function of Pre-strain

DSC heating curves of the samples after different prestraining levels were performed. Figure 4 illustrates the transformation enthalpy versus prestrain. The results indicate that the transformation enthalpy increases almost linearly with the prestrain level. A sample without prestrain displays the maximum transformation enthalpy, which gradually decreases with increasing prestrain level. A lower value of the transformation enthalpy indicates the residual presence of martensitic phase in the Ti-Ni wire, even beyond the A_f temperature. Beyond a prestrain level of

10%, the absorbed enthalpy is almost zero, which means that the martensite remains predominantly present in the Ti-Ni wire and does not transform into the parent phase. We attribute this behavior to the increase in the A_s temperature of oriented martensite, a phenomenon currently under further study.

2.2. Experimental procedure

The epoxy composite of the sample, reinforced with Ti-Ni wires and developed by the authors, has a thickness of approximately 0.4 mm. Fig. 5 illustrates the concept of improving the mechanical properties of the AMF composite. To produce the smart composites, the degassed epoxy mixture was poured into a preheated PTFE mold, in which the Ti-Ni wires had been placed in the grooves.

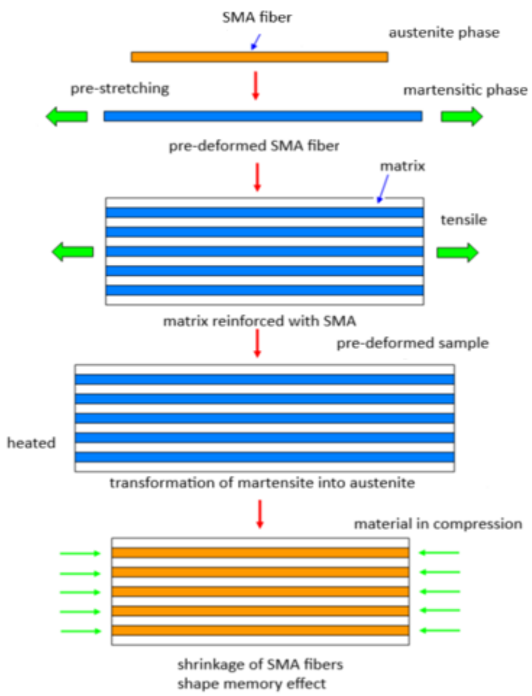

Fig. 5. The smart composite design concept

The smart composites were pre-cured at 80 °C for 2.5 hours and then cured at 150 °C for 2.5 hours [see Fig. 6]. The dried epoxy resin and smart composite samples were sawn to the dimensions required for mechanical testing. The final smart composite had dimensions of 140 × 30 × 0.4 mm³.

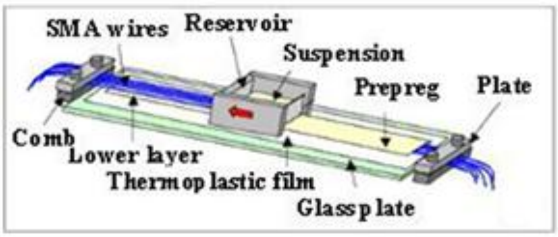

Fig. 6. Fabrication process schematic for the smart composite material

The specimens were shortened to 100 mm and positioned in the clamps of the thermomechanical testing machine [Fig. 7]. The contraction of the SMA wires served to stiffen the specimen and promote the recovery of the stress induced during the application of the load. An experimental study of the mechanical properties was conducted on the manufactured specimens using the Instron 6025 machine, equipped with an axial speed control system.

Fig. 7. Optical image of the smart composite with 30 embedded Ti-Ni wires

Mechanical tests were performed using a machine equipped with a load cell and a capacitive displacement sensor. After heat treatment to stabilize their transformation temperatures, the smart composites allowed experimental determination of the A_s and A_f temperatures. Pull-out tests were also conducted to characterize the critical debonding load and evaluate the strength of the matrix-SMA interface. The tests were carried out at temperatures below A_s and above A_f, allowing the observation of stress-strain curves representative of the stress-induced martensitic transformation. The finite element model was developed and ultimately confirmed by experimental observations.

3. EXPERIMENTAL RESULTS AND DISCUSSIONS

An Instron 6025 universal machine was used to perform tensile testing at different temperatures. To reduce preparation-related bias, at least ten specimens were evaluated for each series. Figure 8 demonstrates nonlinear mechanical behavior, characterized by a maximum strain of 7.15%, fully recovered after unloading. At 40 °C [$T<A_s$], the stress-induced martensitic transformation,accompanied by martensite rearrangement, leads to a strain of approximately 6.9% for a stress of 175 ± 5 MPa. At 90 °C [$T>A_f$], additional tensile tests were performed on the same sample. A_s shown in Figure 6, in the case of a fully austenitic alloy, the initial stress increases rapidly, resulting in a steep stress-strain curve. Once the stress approaches 350 ± 5 MPa, the alloy begins to fail, resulting in a slower increase in stress accompanied by significant deformation.

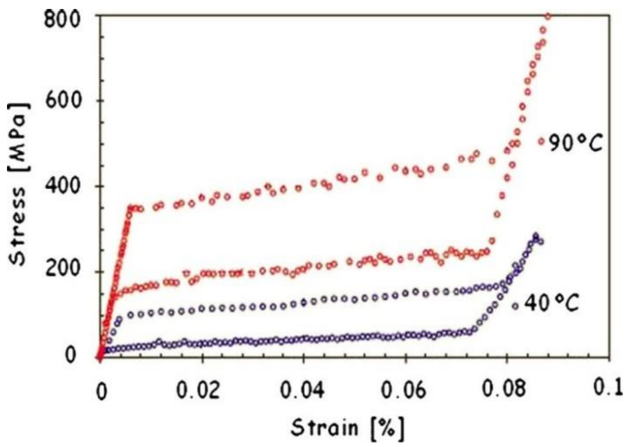

Fig. 8. Axial stress–strain response of a Ti-Ni shape memory alloy subjected to uniaxial tension at temperatures below, within, and above the transformation range (40 °C, 50 °C, and 90 °C)

DOI: 10.65731/ama/2026-0053

Under unloading applied at 475 ± 5 MPa, the stress decreases rapidly in the first phase, then the decrease becomes more gradual when the stress reaches 175 ± 5 MPa. After complete unloading, the deformation is completely absorbed. The deformation disappears completely after unloading. However, the results indicate, according to Fig. 9, that the critical stress σ_m of Ti-Ni wires decreases monotonically with decreasing test temperature, a behavior different from that reported for bulk Ti-Ni alloys. [64, 65] This phenomenon, whose precise cause remains undetermined, is probably related to the specific microstructural texture of the wires, still under analysis.

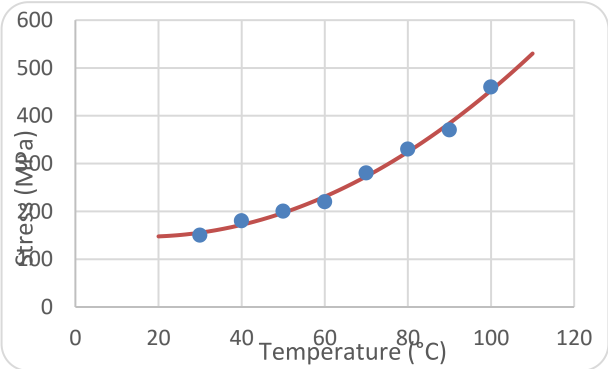

Fig. 9. Dependence of critical stress on temperature for Ti-Ni wires

Tab. 2. Young's modulus of smart composites as a function of temperature

Temperatures [°C]	Young's modulus [GPa]
60	4.4±0.8
80	5.9±0.8
100	7.1±0.8
120	6.9±0.8

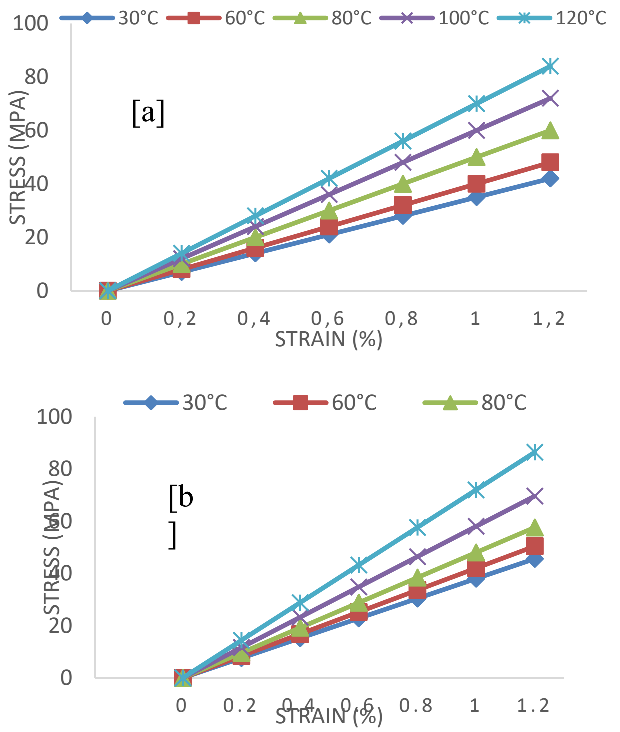

Fig. 10. Comparison of stress-strain curves for the AMF material with pre-stretched fibers at [a] 5% and [b] 10% pre-strain, tested at various temperatures

According to the work of Simoes et al. [69] on a polycrystalline alloy in compression, the critical stress remains constant beyond Af, which has been attributed to the stabilizing effect of residual martensite on the transformation stress in subsequent cycles. Longitudinal tensile tests are presented in Table 2, and typical stress-strain curves are shown in Figure 10. The results show that the Young's modulus of the smart composites varies little with temperature, with the observed difference being limited by the low volume fraction of filaments in the sample. The measured differences are summarized in Table 2.

As highlighted in Figure 8, the epoxy matrix induces a moderate increase in Young's modulus with temperature. This effect is not clearly observable in Table 2, as the values presented correspond to an average over several pre-strain levels. As shown in Figure 11, micrographs of the filament/matrix interface after 12% strain reveal matrix detachment near some filaments. This effect is generally observed in conjunction with matrix cracking and delamination.

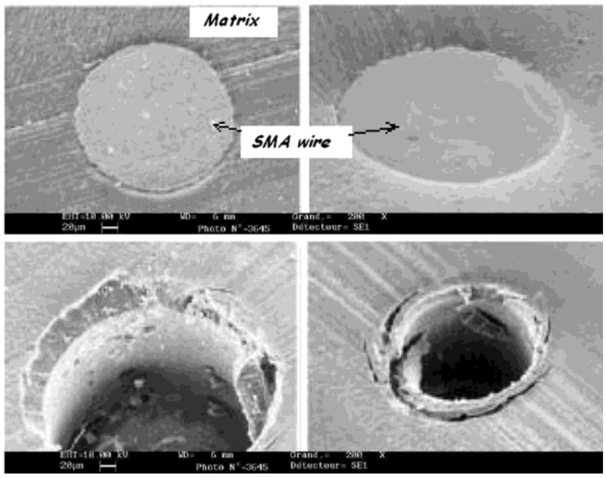

Fig. 11. SEM analysis of the wire/matrix interface evolution with increasing pre-strain: [a] Initial state; [b] Localized matrix deformation at 8% pre-strain; [c] Initiation of SMA wire tearing at 10% pre-strain; [d] Severe interfacial degradation at 12% pre-strain

4. NUMERICAL MODELING AND INTERPRETATION OF RESULTS

4.1. Numerical simulation methods

To reduce the computational cost while maintaining an accurate representation of the overall mechanical behavior of the composite, several simplifying assumptions were adopted. The epoxy matrix was assumed to be homogeneous, isotropic, and linearly elastic within the investigated loading range. The Ti–Ni wires were modeled using a phenomenological constitutive law capable of reproducing stress-induced martensitic transformation and superelastic behavior. In this initial modeling framework, matrix plasticity, progressive damage, functional fatigue, and residual stresses arising from the manufacturing process were not considered [70].

The reduced numerical models developed by Annadata et al. [71] have made it possible to considerably reduce the computational cost of laminates incorporating SMA wire networks, while maintaining satisfactory accuracy. In their study, they consider fully nonlinear stress distributions and introduce a thorough phenomenological model of the constitutive hysteretic behavior of SMA. It has been shown that this approach significantly reduces the computational cost compared to high-fidelity FEA, while maintaining satisfactory accuracy, with the root mean square error remaining below 10%.

The behavior was analyzed using a nonlinear finite element method based on the von Kármán strain–displacement relationship. A finite element approach was developed by Khorramabadi et al. [72] to analyze the buckling behavior of a rectangular laminated plate. Particular importance was given to the role of the SMA wire distribution function. Thus, a non-uniform distribution of SMA wires is more effective in increasing the buckling resistance of the plate. Markuszewski et al. [73] studied the nonlinear transient finite element analysis of a single-ended plate actuator made of a thermally activated elastomer-SMA composite based on a displacement model. Asgari et al. [74] applied the finite element method to model the geometrically nonlinear behavior of a panel reinforced with SMA wires, based on von Kármán's large deformation theory. Based on the ABAQUS code.

Finite element simulations with LS-Dyna® were performed to investigate the superelastic response of Ti–Ni SMA. Experimental data recorded during tensile tests on the SMA wires were used to determine the stress–strain curves. Table 3 summarizes the average results in terms of uniaxial engineering response. The sample consists of a thin plate measuring 30×100×0.4 mm³, incorporating 30 wires [Ø 0.2 mm, length 100 mm], subjected to a longitudinal force of 10 N applied at one end while the other is fixed.

Tab. 3. Material parameters used in the model

Phase	Austenite phase	Martensite phase
Density	4.5	4.5
Young's modulus [MPa]	58334	25000
Poisson's ratio	0.3	0.3
σ^{f}_{AS} [MPa]	350	175
σ^{s}_{AS} [MPa]	475	100
σ^{f}_{SA} [MPa]	250	60
σ^{s}_{SA} [MPa]	175	25
ε_L [%]	0.06	0.06
α	0	0

The constitutive parameters of the proposed model were identified from experimental tests performed on both the Ti–Ni wires and the composite specimens. The elastic moduli, transformation stresses, and parameters governing the superelastic response were determined from the experimentally obtained stress–strain curves. An iterative calibration procedure was subsequently employed to minimize the discrepancy between the numerical predictions and the experimental observations. The quality of the calibration was assessed based on the initial elastic slope, the transformation plateau, and the overall stiffness of the composite specimens [75].

The 3D FE model has a total of 1,554,200 elements for the matrix, plus 192,000 elements corresponding to the 30 wires. The matrix and wires were meshed using the SOLID45 solid element. A higher mesh density was adopted in the wire/epoxy matrix contact region to ensure a better representation of the interaction. In order to obtain a reliable estimation of the behavior of the matrix/wire contact area, which is particularly sensitive to delamination phenomena, the mesh was refined locally. It becomes coarser as one moves away from the interface, as shown in Figure 12.

The load transfer between the Ti–Ni wires and the epoxy matrix was modeled through a frictional contact interface. The interfacial adhesion coefficient employed in the simulations was initially estimated from experimental observations and subsequently calibrated to ensure good agreement between numerical predictions and experimental measurements. Although simplified, this modeling strategy captures the main load-transfer mechanisms occurring at the wire–matrix interface while preserving the numerical robustness and stability of the finite element analysis.

Fig. 12. Mesh of the structure at the fixed boundary

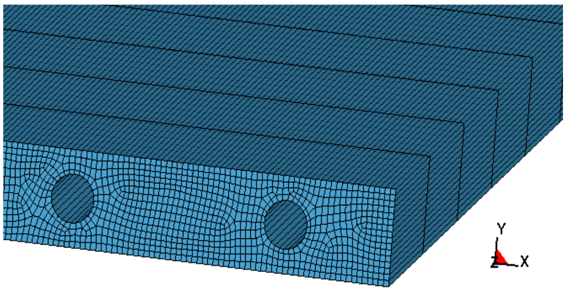

In the modeling, the SMA wires are defined as slave surfaces and the matrix as the master surface, taking into account the friction at the interface. The interaction between the two phases was simulated using the contact_2D_automatic_surface_to_surface option available in LS-Dyna®. The finite element simulations were carried out to evaluate the qualitative mechanical response of the SMA/epoxy composite system.

The boundary conditions were defined to accurately replicate the experimental configuration employed during the tensile tests. One end of the specimen was fully fixed, whereas a prescribed axial displacement was progressively applied at the opposite end. The transverse degrees of freedom were constrained to eliminate rigid-body motions and ensure numerical stability. This approach provided a direct correspondence between the finite element simulations and the experimental setup, thereby facilitating a reliable assessment of the model's predictive capability through comparison with the measured mechanical response [76].

A longitudinal load of 10 N was applied to the upper surface of the specimen, while the lower surface was rigidly constrained by a recessed boundary condition [see Fig. 13].

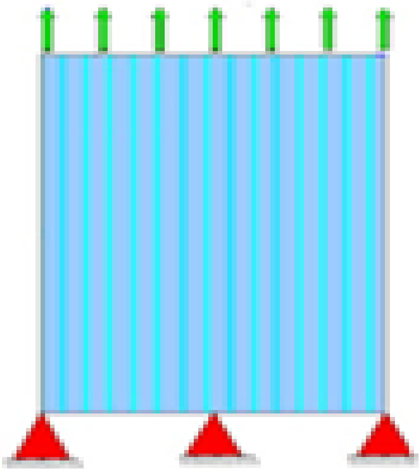

Fig. 13. Specification of the plate geometry and constraint conditions

 DOI: 10.65731/ama/2026-0053

4.2. Numerical results and discussions

The aim of this experiment was to determine the tensile modulus of Ti–Ni wires under two different conditions. The modulus was evaluated in the martensitic phase [at a temperature below A_s] and in the austenitic phase [at a temperature above A_f]. When the temperature drops below the martensite finish temperature [M_f], the material becomes fully martensitic. In this phase, multiple variants and twins are present. No transformation to austenite occurs as long as the temperature remains below the austenite start temperature [A_s].

In this phase, the material exhibits multiple variants and twinning. No transformation to austenite occurs as long as the temperature remains below the austenite start temperature [A_s]. However, under loading, the material first deforms elastically. Once the stress exceeds a critical level, martensitic twin pairs start to detwin and reorient into stress-preferred variants. During this reorientation process, the stress increases only slightly.

This single martensitic variant remains thermodynamically stable at temperatures below As. Consequently, during unloading, no transformation into multivariant martensite occurs, and only a minor reversible elastic strain is observed. When the temperature exceeds the martensite start temperature, the alloy is in the austenitic phase. Under loading at an ambient temperature above the austenite finish temperature [A_f], the SMA exhibits a linear elastic response governed by the elastic modulus of the austenite.

Mechanical loading exceeding the critical stress triggers the transformation of austenite into stress-induced [detwinned] martensite.

Upon completion of the stress-induced martensitic transformation, the mechanical behavior is governed by the linear elastic deformation of the self-accommodated [twinned] martensite. Under un-loading, an evident hysteresis behavior is observed, associated with the reverse martensite–austenite transformation, resulting in the full recovery of the residual strain in the shape memory alloy. Numerical analyses were also conducted using the explicit FE code LS-Dyna®, where the tensile SMA specimen was modeled by means of the MAT_SHAPE_MEMORY material model. It represents the superelastic response of the shape memory alloy, defined by the capability of the material to experience substantial deformation and subsequently return to its original configuration after a full loading–unloading cycle (see Fig. 14):

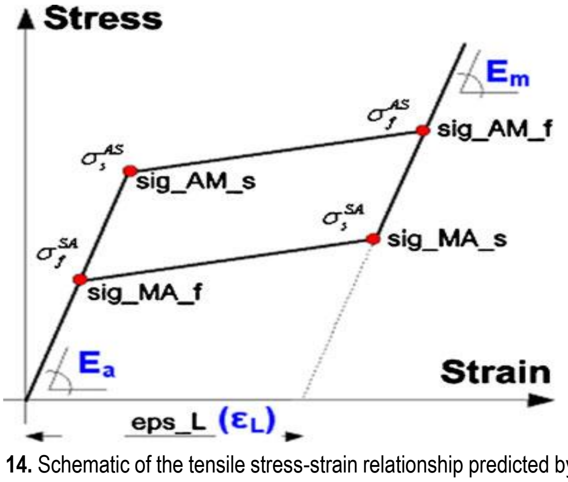

Fig. 14. Schematic of the tensile stress-strain relationship predicted by the superelastic shape memory alloy constitutive model

In Fig. 15a, b, the simulated responses are compared to the experimental tensile test results of the SMA specimen, thereby verifying the validity of the adopted finite element model. As illustrated in Fig. 13, the model incorporating the presented thermomechanical parameters provides a reliable prediction of the pseudoelastic behavior of the shape memory alloy.

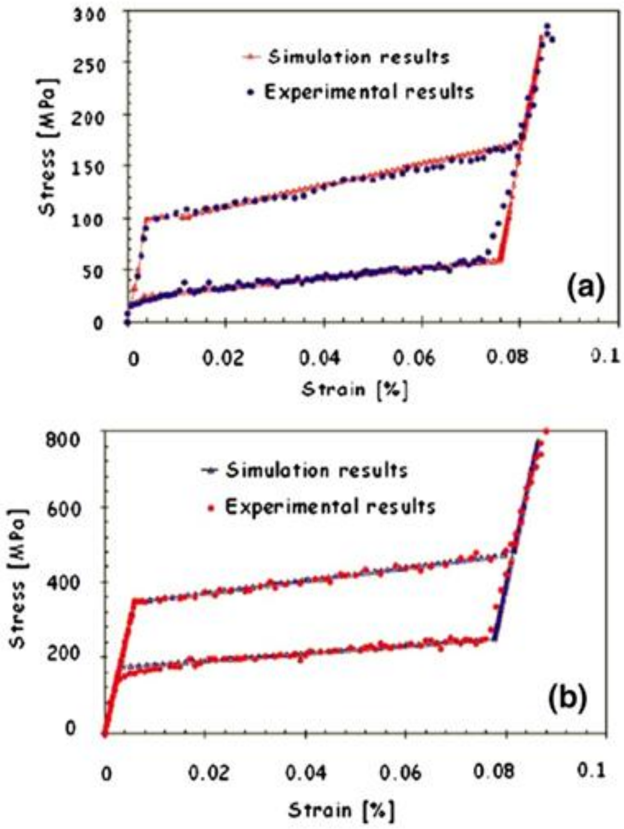

Fig. 15. Experimental and numerical results for the SMA sample at two temperatures: [a] 40 °C, below A_s, and [b] 90 °C, above A_f

For instance, the simulated martensitic transformation start and finish stresses, 352 ± 2 MPa and 478 ± 2 MPa, exceed the experimental values by a small margin. Conversely, the corresponding start and finish stresses of the reverse transformation are 244 ± 2 MPa and 182 ± 2 MPa. The simulated elongation values for the specimen, corresponding to the conditions of 100% initial austenite and 100% initial martensite, were found to be 0.1% and 0.4%, respectively, which are greater than those measured experimentally. The analysis focused on the stress distribution and displacement fields in the integrated SMA actuators, as well as the resulting in-plane actuation force of the smart composite specimen, considering different boundary conditions.

The results presented in Figures 16 and 17 indicate that the tensile data obtained from smart composite specimens at temperatures below the austenite start [As] or above the austenite finish [Af] correspond to the martensitic and austenitic phases, respectively. The displacement field in the wire loading direction differed according to the phase of the material, whether martensitic or austenitic. Under increasing load, the specimens deformed elastically, showing an elastic response with higher stiffness. The numerical findings demonstrate that integrating active wires in the austenitic state provides the optimal configuration for enhancing the global behavior of the Ti–Ni/epoxy composite. When electrical resistance heating is applied, the Ti–Ni wires contract as a result of the martensite-to-austenite phase transformation. It was found that composites incorporating prestrained SMA wires achieve superior levels of reversible strain, along with improved mechanical and physical performance.

More importantly, they are capable of producing extremely high recovery stresses, which are critical for structural applications. It was demonstrated that the contraction of the actuated SMA wire produces compressive loading in the beam matrix, resulting in decreased structural displacements. Les résultats ont indiqué que la transformation induite dans la fibre SMA réduit significativement la contrainte axiale. La principale limite de cette approche est que la fixation des fils SMA à la surface de la matrice peut avoir peu d'application pratique aux structures composites polymères. En effet, un chauffage du fil Ti-Ni proche de la température de transition vitreuse de la matrice peut entraîner un ramollissement et une fragilisation de l'interface matrice-fil SMA. Nous avons tout intérêt à traiter thermiquement les fils pour obtenir des températures martensitiques largement inférieures à la température de transition vitreuse de la matrice.

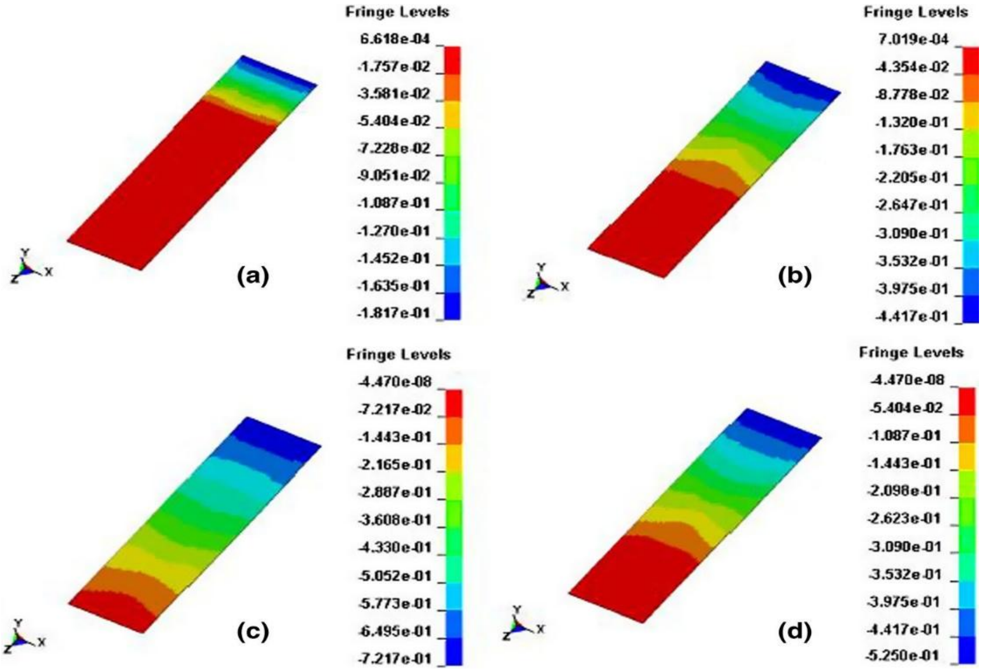

Fig. 16. Sequential displacement fields [z-z direction] demonstrating the structural response of the austenitic Ti-Ni/epoxy composite at selected time intervals: [a] 6 s, [b] 21 s, [c] 37 s, and [d] 53 s

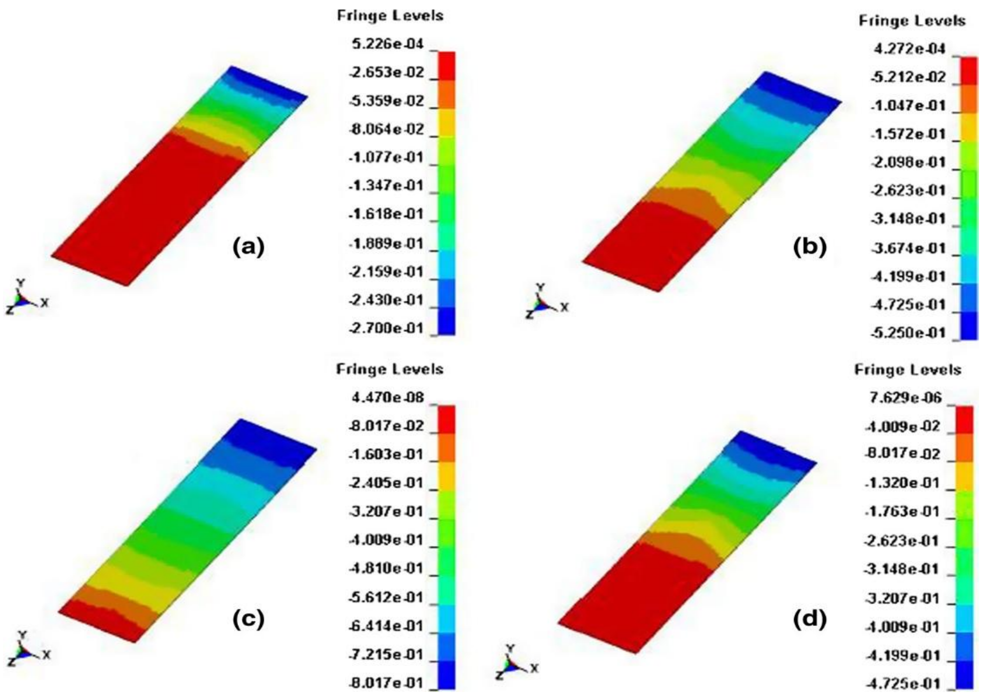

Fig. 17. Sequential displacement fields [z-z direction] demonstrating the structural response of the martensitic Ti-Ni/epoxy composite at selected time intervals: [a] 6 s, [b] 21 s, [c] 37 s, and [d] 53 s

4.3. Experimental Validation of the Numerical Model

The validation of the proposed model was not limited to a qualitative comparison of the stress–strain curves. It also considered the model's ability to accurately reproduce the initial elastic slope, the onset of martensitic transformation, the superelastic plateau, and the overall stiffness observed experimentally. The satisfactory agreement obtained for these key mechanical features demonstrates the predictive capability of the model within the loading range investigated.

In this section, representative numerical simulations are provided to demonstrate the qualitative behavior of smart composite responses. Model validation was carried out through a set of simulations in which the constitutive parameters correspond to those listed in Tables 1 and 3. The tensile test results of smart composite specimens, comparing experimental data with finite element simulations, are reported in Figure 18. A linear behavior was observed in the specimen, reflecting the primary contribution of the linear elastic fibers. To improve the accuracy of the simulations, debonding effects were considered in the numerical model according to the experimental observations.

A bonding factor of 0.8 was incorporated into the numerical model to match the experimental findings. This adjustment demonstrates that the finite element formulation is capable of reliably capturing the elastic behavior of the composites, with an overall error margin of around 1% compared to the experimental measurements.

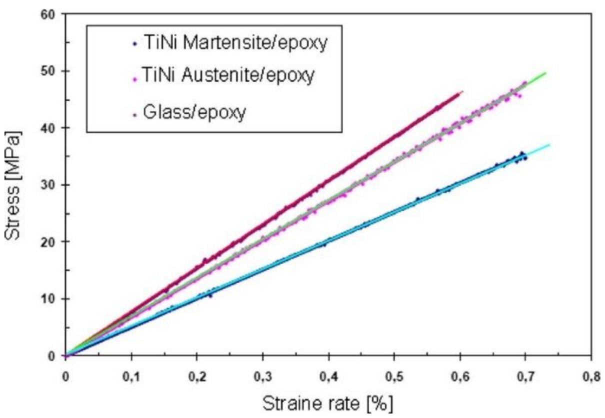

Fig. 18. Experimental vs. simulated tensile response of thin active composites: a glass/epoxy case study

5. LIMITATIONS OF THE PRESENT STUDY AND FUTURE RESEARCH DIRECTIONS

The present study was deliberately limited to the analysis of the mechanical behavior of shape memory alloy (SMA) wire-reinforced hybrid composites under monotonic loading conditions. This approach was adopted to develop, calibrate, and validate the proposed numerical model using experimental results representative of the initial mechanical response of the composites. Although this methodology enables an accurate assessment of the mechanical performance under the considered loading conditions, it does not capture certain phenomena intrinsically associated with SMAs, such as full hysteretic behavior, functional fatigue, the evolution of transformation stresses during cyclic loading, the stability of superelastic properties, or the progressive degradation of the wire–matrix interface. These mechanisms play a critical role in applications involving repeated loading or long-term service conditions. Their investigation will require dedicated cyclic experimental tests as well as the development of a more advanced numerical framework capable of accounting for these effects.

6. CONCLUSION

This study presents an integrated experimental–numerical approach for investigating the thermomechanical behavior of intelligent hybrid composites reinforced with Ti–Ni shape memory alloy (SMA) wires. This research is devoted to studying the thermomechanical performance of SMA wire–reinforced polymer composites under a range of operating conditions. The primary characteristics of SMAs—namely, the shape memory effect and pseudoelastic response—were simulated using a macroscopic phenomenological model. The stress–strain response of a composite plate containing shape memory alloy wires is illustrated and analyzed. Composite specimens with embedded SMA wires subjected to different pre-strain levels were successfully manufactured.

In composites made of an epoxy matrix reinforced with shape memory alloy [SMA] wires, the SMA elements play a decisive role in the overall mechanical behavior, as the martensitic transformation of the wires generates a plateau effect that directly influences the slope of the stress-strain curve. Pre-deformation strongly affects the composite's stress-strain response under normal and transverse shear stresses.

The results suggest that, for the configurations and loading conditions investigated, the incorporation of SMA wires can contribute to improved load transfer and a more favorable mechanical response of the hybrid composite. The actuator deformation in various actuation modes was modeled using a simplified finite element approach. The numerical results show good agreement with the experimental measurements under the monotonic loading conditions investigated. This agreement confirms the ability of the proposed model to reproduce the initial mechanical response of the hybrid composites considered. However, the present validation remains limited to the loading conditions examined in this study and should be extended through further investigations involving cyclic loading, more complex thermomechanical effects, and larger-scale structures in order to broaden the applicability of the model.

The results obtained demonstrate that the proposed numerical model can accurately reproduce the mechanical behavior of Ti–Ni wire-reinforced hybrid composites within the range of monotonic loading conditions investigated. The good agreement between numerical predictions and experimental observations confirms the suitability of the proposed approach for describing the initial mechanical response of these smart composite structures. The present work constitutes a first step toward a more comprehensive understanding of SMA-reinforced hybrid composites. Future studies will focus on cyclic loading effects, functional fatigue, wire–matrix interface durability, and model validation under more complex thermomechanical loading conditions. Addressing these aspects will be essential for improving the assessment of long-term reliability and extending the applicability of smart composite systems in engineering applications.

REFERENCES

1. Topel-Zeren E, Akşit A, Aydoğdu Y. Shape memory effect of polymeric composite materials filled with NiMnSbB shape memory

alloy for textile materials. Materials Research Express. 2020; 7(5): 055702. https://doi.org/10.1088/2053-1591/ab8c6e

2. Zarek M, Layani M, Cooperstein I, Sachyani E, Magdassi S. 3D Printing of Shape Memory Polymers for Flexible Electronic Devices. Advanced Materials. 2026; 28(22):4449-4454. https://doi.org/10.1002/adma.201701627
3. Rodinò S, Curcio EM, Di Renzo A, Sgambitterra E, Magarò P, Furgiuele F, Brandizzi M, Maletta C. Shape Memory Alloy-Polymer Composites: Static and Fatigue Pullout Strength under Thermo-Mechanical Loading. Materials. 2022;15(9):3216. https://doi.org/10.3390/ma15093216
4. Sahli M, Necib B. Characterisation and modelling of behaviour of a shape memory alloys. Int J Adv Manuf Technol.2014; 70:1847–1857.
5. Necib B, Guarbi A, Lebied A, Sahli M. The Smart materials and their applications in the engineering fields. IEEE; 2015. https://doi.org/10.1109/NSITNSW.2015.7176419
6. Brandizzi M, Maletta C. Shape Memory Alloy-Polymer Composites: Static and Fatigue Pullout Strength under Thermo-Mechanical Loading. Materials. 2022; 15(9): 3216. https://doi.org/10.3390/ma15093216
7. Salowitz N, Misra S, Haider MI, Povolo M, Rohatgi P. Investigation into the Performance of NiTi Shape Memory Alloy Wire Reinforced Sn-Bi Self-Healing Metal Matrix Composite. Materials. 2022; 15(9):2970.
8. Yongji L, Jianping L, Yao X, Junying M. Effects of cold-drawing and low-temperature annealing on the sensing properties of NiTi alloys. Materials Research Proceedings; 2023.
9. Helbert G, Dieng L, Chirani SA, Pilvin P. Influence of the thermomechanical behavior of NiTi wires embedded in a damper on its damping capacity: Application to a bridge cable. AIMS Materials Science. 2023; 10(1):1-25.
10. Sun P, Wang Q, Feng J, Ji P, Zhang J, Yin F. Effect of Nb on the Damping Property and Pseudoelasticity of a Porous Ni-Ti Shape Memory Alloy. Materials. 2023; 16(14):5057.
11. Mohammed MK, Al-Ahmari et al. Laser-Machining of Microchannels in NiTi-Based Shape-Memory Alloys. Materials; 2020.
12. Karelin R et al. Structure and Properties of TiNi Shape Memory Alloy after Thermomechanical Treatment. Metals; 2023.
13. Scholtes D, Seelecke S, Motzki P. Electro-Thermo-Mechanical Characterization of Shape Memory Alloy Wires for Actuator and Sensor Applications - Part 1; 2024.
14. Milleret A et al. 4D printing of Ni–Mn–Ga magnetic shape memory alloys. Smart Materials and Structures; 2022.
15. Shreekrishna S et al. A review on shape memory alloys and their prominence in engineering; 2023.
16. Liu Y, Zhang C. Effects of interlayer on microstructure and mechanical properties of titanium/steel joints: a short review. Metals; 2024.
17. Roman Ka, Victor Ko et al. Structure and Properties of TiNi Shape Memory Alloy after Quasi-Continuous Equal-Channel Angular Pressing in Various Aged States. Metals; 2023.
18. Eggeler G, Frenzel J, Pons J. Particles in Shape Memory Alloys Revisited: Effects on Functional and Structural Properties. Shap. Mem. Superelasticity. 2025;11:350–362.
19. Shreekrishna S et al. A review on shape memory alloys and their prominence in automotive technology. Journal of Intelligent Material Systems and Structures; 2023.
20. Zubair Z et al. Thermal activation and dynamic mechanical behaviour in shape-memory composites for medical applications. » Textile Research Journal Pages. 2025; 1902-1912.
21. Dong L, Mann W, He B. [2025]. Influence of Cu on the mechanical and shape memory properties of TiNi alloys. Materials. 2025; 18(10): 2407.
22. Chen LY et al. An overview of additively manufactured metal matrix composites. Manufacturing Review. 2024; 11: 1–26.
23. Ibrahim BM [2023]. A review on comparison between NiTi-based and Cu-based shape memory alloys. Materials Research Express. 2023; 10(5):055505.
24. Om H et al. Fabrication and characterization of vacuum induction melted NiTi shape memory alloys. Transactions of Nonferrous Metals Society of China. 2025; 35(4): 1021–1031.
25. Ozair H et al. Shape memory hybrid composites: SMA wire-stitched composites and their damage recovery. ACS Omega. 2022;7(27): 24015–24026.
26. Scholtes D, Seelecke S, Motzki P. Electro-thermo-mechanical characterization of shape memory alloy wires for actuator and sensor applications-Part 1. Advanced Engineering Materials. 2024;26(2): 2300567.
27. Twala B, Kaur H, Thakur A, Gupta L R, Dogra S, Singh R. A review of shape memory alloy applications and future trends in the aerospace industry. Smart Materials and Structures. 2024;33: 045028.
28. Behvar A et al. Insights into the future of manufacturing and designing NiTi-Cu shape memory alloys via binder jet additive manufacturing. Mechanics of Advanced Materials and Modern Processes. 2025; 11: 1–21.
29. Relevant Choices Affecting the Fatigue Analysis of Ni-Ti Endovascular Devices. Materials. 2023;16(8):3178.
30. The Effect of Intraoral Thermal Changes on the Mechanical Behavior of Nickel-Titanium Wires: An In-Vitro Study. Cureus. 2024; 16(10): e72207.
31. Yang C et al. Role of point defects in stress-induced martensitic transformation in NiTi shape memory alloys. Physical Review B. 2022; 105: 144108.
32. Wang Z et al. Strain rate effect on the thermomechanical behavior of NiTi SMAs: experiments and modelling. Metals. 2022; 13(1): 58.
33. He B. et al. Comprehensive shape memory alloys constitutive models and their application in hybrid composites. Composite Structures. 2023; 316: 114036.
34. Sakhaei AH et al. Microscale investigation of phase transformation and irrecoverable strain in NiTi shape memory alloys. Mechanics of Materials. 2023; 181: 104337.
35. Rao Z et al. A three-dimensional constitutive model for shape memory alloys under multiaxial loading. International Journal of Solids and Structures. 2023; 273-274: 112349.
36. Dutta S, Sarma DK, Choudhari R, Khanna S. [2025]. A State-of-the-Art Review on Micro-Machining of Nitinol Shape Memory Alloys and Optimization of Process Variables Considering the Future Trends. Manufacturing. 2025; 9(6): 183.
37. Mohammadgholipour, A et al. Mechanical properties and constitutive models of shape memory alloys. Smart Materials&Structures. 2023; 32(10): 105009.
38. He B et al. Comprehensive shape memory alloys constitutive models and their application in hybrid composites. Composite Structures. 2023; 316: 114036.
39. Sakhaei AH et al. Microscale investigation of phase transformation and irrecoverable strain in NiTi shape memory alloys. Mechanics of Materials. 2023; 181: 104337.
40. Xie X et al. Phase-field damage simulation of sub-loop loading in TiNi shape memory alloys. Theoretical and Applied Fracture Mechanics. 2024; 126: 103733.
41. Gangil N, Siddiquee AN, Mufazzal S, Muzakkir S, Maheshwari S. Shape Memory Alloy Based NiTi Reinforced Functionally Graded Material for Vibration Damping. J. Mater. Des. Appl. 2021; 235: 2771-2782.
42. Ozair H, Wang Y, Mandal P, Roy S. Shape Memory Hybrid Composites: SMA Wire-Stitched Composites and Their Damage Recovery. ACS Omega. 2022; 7(27): 24015-24026.
43. Li H, Wang J, Sun Q. Phase transformation and recovery behavior of NiTi-based composites studied by in situ neutron diffraction. Acta Materialia. 2022; 237: 118126.
44. Huang C, Kim JY, Zhang Y. Microscale plasticity and superelasticity of NiTi shape memory alloys investigated via nanoindentation and TEM. Scripta Materialia. 2023; 232: 115488.
45. Rao VS, Suresh, K. Thermomechanical response of TiNi/Al6061 composites processed by spark plasma sintering. Journal of Alloys and Compounds. 2021; 853: 157117.
46. Patel R, Sharma R, Singh D. Experimental and numerical

DOI: 10.65731/ama/2026-0053

investigation of NiTi/polymer shape memory composites under cyclic deformation. Journal of Composite Materials. 2022; 56(19): 2823–2838.
47. Zhang W, Liu H, Fang Y. Nonlinear vibration behavior of SMA fiber-reinforced laminated composite plates under large amplitude loading. Chinese Journal of Aeronautics. 2020; 33(8): 2337–2347.
48. Alam S, Rahman M, Chowdhury M. Mechanical and damping properties of carbon/epoxy composites embedded with NiTi shape memory wires. Composites Part A: Applied Science and Manufacturing. 2024; 179: 107611.
49. Khan N, Singh P, Yadav R. [2023]. Thermo-mechanical bending behavior of hybrid composites integrating SMA and SMP layers. Smart Materials and Structures. 2023; 32(9).
50. Gao L, Ren J, Li X. Design and characterization of novel shape memory alloy actuators for soft robotics applications. Journal of Intelligent Material Systems and Structures. 2022; 33(5): 587–600.
51. Tabrizikahou A et al. A review of shape memory alloy fiber-reinforced concrete composites: from experimental testing to computational modelling. Composites Part B: Engineering. 2024; 301: 131243.
52. Xue J, Lee S. Nonlinear post-buckling of shear deformable smart composite beams embedded with SMAs. Smart Materials and Structures. 2025; 34(1): 015025.
53. Mandolino M, Scholtes D, Ferrante F, Rizzello G. A physics-based hybrid dynamical model of hysteresis in polycrystalline shape memory alloy wire transducers. Smart Materials and Structures. 2023; 32(10): 105009.
54. Yuan G, Bai Y, Jia Z, Hui D, Lau K-T. Enhancement of interfacial bonding strength ofSMA smart composites by using mechanical indented method. Composites Part B: Engineering. 2016; 106: 99–106.
55. Lagoudas DC (Ed.). Shape Memory Alloys: Modeling and Engineering Applications. Springer New York; 2008.
56. Sgambitterra E, Curcio E, Rodinò S, Renzo D, Magarò P, Furgiuele F, Maletta C, Shape memory alloys-polymer composites: interfacial strength under mechanical and thermal loading. Procedia Structural Integrity; 2021.
57. Carpinteri A, Di Cocco V, Fortese G, Iacoviello F, Natali S, Ronchei C, Scorza D, Vantadori S, Zanichelli A. Mechanical behaviour and phase transition mechanisms of a shape memory alloy by means of a novel analytical model. Acta Mechanica et Automatica. 2018; 12(2): 105–108.
58. Rodinò S, Curcio EM, Renzo DA, Sgambitterra E, Magarò P, Furgiuele F, Brandizzi M, Maletta C. Shape memory alloy–polymer composites: Static and fatigue pullout strength under thermo-mechanical loading. Materials. 2022; 15(9): 3216.
59. Rodinò S, Maletta C. Multiphysics modeling and optimization of an innovative shape memory alloy–polymer active composite. Polymer. 2024; 307: 127316.
60. Otsuka K, Ren X. Physical metallurgy of Ti–Ni-based shape memory alloys. Progress in Materials Science. 2005; 50: 511–678.
61. Miyazaki S, Kimura S, Hosoda H. Development and characterization of NiTi shape memory alloys. Materials Science and Engineering A.
62. Rodinò S, Curcio EM, Renzo DA, Sgambitterra E, Magarò P, Furgiuele F, Maletta C. Shape memory alloy—polymer composites: Static and fatigue pullout strength under thermo-mechanical loading. Materials; 2022.
63. Daghash SM, Ozbulut OE. Characterization of superelastic shape memory alloy fiber-reinforced polymer composites under tensile cyclic loading. Materials&Design. 2016; 111: 504–512.
64. Hartl DJ, Lagoudas DC. Aerospace applications of shape memory alloys. Proceedings of the Institution of Mechanical Engineers. Part G: Journal of Aerospace Engineering. 2007; 221: 535–552.
65. Song G, Ma N, Li HN. Applications of shape memory alloys in civil structures. Engineering Structures. 2006; 28: 1266–1274.
66. Brinson LC. One-dimensional constitutive behavior of shape memory alloys. Journal of Intelligent Material Systems and Structures. 1993; 4: 229–242.
67. Zhang, Z, Liu Y. Thermomechanical behaviour of SMA reinforced smart composites: Numerical and experimental approaches. Smart Materials and Structures; 2024.
68. Rodinò S, Curcio EM, Sgambitterra E, Maletta C. SMA-polymer composite made by 3D printing: modelling and experiments. Procedia Structural Integrity; 2023.
69. Simoes M, Martínez-Pañeda E. Phase-field modelling of fracture and fatigue in shape memory alloys. International Journal of Plasticity. 2020;134:102777.
70. Bollas D, Pappas P, Parthenios J, Galiotis C. Stress generation by shape memory alloy wires embedded in polymer composites. Acta Materialia. 2007; 55(16): 5489–5499, 2007.
71. Annadata AR et al. [2024]. Investigation and validation of a shape memory alloy material model for smart composite structures. Materials. 2024; 17(5): 1163.
72. Khorramabadi R et al. Post-buckling and vibration analysis of double-curved sandwich plates with SMA-reinforced hybrid composite face sheets. Composite Structures. 2023; 314: 114647.
73. Markuszewski D, Wądołowski M, Krajewski A. The Influence of Variable Stiffness of the Shape Memory Alloys Carbon Composite Structure on Mechanical Vibration. Materials. 2024; 17(2): 480.
74. Asgari M, Mohammadimehr M, Arabzadeh-Ziari M, Arabzadeh-Ziari E. Static bending, vibration, and buckling responses of a sandwich beam composed of five layers including SMA particles. Mechanics of Advanced Composite Structures. 2025; 12(1) 153-168.
75. Rodinò S, Maletta C. Multiphysics modeling and optimization of an innovative shape memory alloy-polymer active composite. Polymer; 2024.
76. Lelieveld C, Jansen K, Teuffel P. Mechanical characterization of a shape morphing smart composite with embedded shape memory alloys in a shape memory polymer matrix. Journal of Intelligent Material Systems and Structures. 2016; 27(15): 2038–2048.

We gratefully acknowledge the support provided by the Applied Mechanics Department at the Femto-st Institute in Besançon, France.

Abdelaziz Lebied: https://orcid.org/0000-0002-2588-1161

Sidali Bacha: https://orcid.org/0000-0003-2765-3952

Houssam Lala: https://orcid.org/0009-0000-8250-0698

Mohamed Lakhdar Sahli: https://orcid.org/0000-0002-8690-5366